Computational projects with the Landau–Zener problem in the quantum mechanics classroom ⊘

Livia A. J. Guttieres; Marko D. Petrović; James K. Freericks

Check for updates

CHORUS

View Online   Export Citation

Articles You May Be Interested In

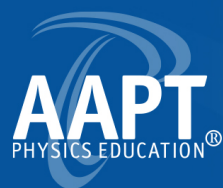Bell-state generation in circuit QED via Landau-Zener tunneling

AIP Conf. Proc. (July 2007)

Model study of the Landau–Zener approximation

Am. J. Phys. (November 2005)

Landau–Zener type surface hopping algorithms

J. Chem. Phys. (June 2014)

Computational projects with the Landau–Zener problem in the quantum mechanics classroom

Livia A. J. Guttieres[a)]
Department of Physics, University of Chicago, 5720 South Ellis Avenue, Chicago, Illinois 60637

Marko D. Petrović[b)] and James K. Freericks[c)]
Department of Physics, Georgetown University, 37th and O Sts. NW, Washington, DC 20057

The Landau–Zener problem, where a minimum energy separation is passed with constant rate in a two-state quantum-mechanical system, is an excellent model quantum system for a computational project. It requires a low-level computational effort, but has a number of complex numerical and algorithmic issues that can be resolved through dedicated work. It can be used to teach computational concepts, such as accuracy, discretization, and extrapolation, and it reinforces quantum concepts of time-evolution via a time-ordered product and of extrapolation to infinite time via time-dependent perturbation theory. In addition, we discuss the concept of compression algorithms, which are employed in many advanced quantum computing strategies, and easy to illustrate with the Landau–Zener problem. © *2023 Published under an exclusive license by American Association of Physics Teachers.*
https://doi.org/10.1119/5.0139717

I. INTRODUCTION

The Landau–Zener problem is an exactly solvable problem in quantum mechanics that describes how a quantum particle tunnels between two states as a function of the speed with which it traverses an avoided crossing.[1,2] The exact solution involves mapping the time-dependent Schrödinger equation onto the so-called Weber equation, which is solved with parabolic cylinder functions. However, because these functions are not so familiar to most students, this mapping is rarely taught. Instead, because the system is just a two-state system, one can compute the results numerically. This brings in issues related to discretization and to accuracy, which can be particularly acute for high accuracy because the solution has slowly decaying oscillations that make determining the final tunneling probability challenging without invoking some form of averaging. Instead, one can use time-dependent perturbation theory to append the long-time results and achieve much higher accuracy solutions.

This makes the Landau–Zener problem an excellent choice for a computational project in a quantum mechanics class. The time evolution, via a Trotter product formula, is easy to code. Appending the time evolution at long times requires a mastery of time-dependent perturbation theory and the interaction representation. Modifying the discretization size and the time cutoff for the time evolution allows students to understand issues related to the accuracy of the computation. Finally, this specific problem has a few different compression strategies that can be employed—these strategies replace the product of a string of operators by a single operator exactly equal to the product. Compression strategies are employed in quantum computing to reduce the depth of a quantum circuit.[3,4] Here, one can learn how such compression strategies work and how to parameterize SU(2) rotations in two different ways to complete the compression.

In this work, we describe a student-led project on the Landau–Zener problem that will enable students to learn many of these different topics related to quantum mechanics and computation. This can be achieved even with beginner to intermediate competency with programming because the codes required are quite simple to implement. It also provides a nice mix between formal development and computational work, similar to much of contemporary research.

The Landau–Zener problem was originally solved in 1932 by Landau,[1] Zener,[2] Stueckelberg,[5] and Majorana.[6] We also have found it discussed in two textbooks: Konishi and Pafutto[7] and Zweibach.[8] Interestingly, the Landau–Zener problem is not widely discussed in other quantum mechanics textbooks, even though it is ubiquitous in modern physics. Historically, it was initially applied to inelastic atomic and molecular collisions. Beyond collisions, two-level systems that exhibit nonadiabatic transitions include Rydberg atoms in rapidly rising electric fields, qubit states in an NV center in diamond, and double-quantum dots. Other systems include qubits based on Josephson junctions, charge qubits in semiconductor quantum dots, graphene devices with an avoided crossing near the Dirac point, ultracold molecules in a laser trap, and even time-resolved photoemission in charge-density-wave systems. A discussion of many of these applications is given in a recent review article.[9]

The problem has also been discussed in the pedagogical literature. One study explores the accuracy of Runge–Kutta integration of the Schrödinger equation,[10] while another uses the Landau–Zener approximation,[11] which turns out not to be very accurate. The problem is mapped to the problem of a sphere rolling without slipping[12] and solved classically, and it is also solved using a simple conceptual approximation that averages probabilities, not probability amplitudes, due to the fast oscillations.[13] Finally, another approach uses contour integrals.[14] Our work focuses on developing a computational project that employs perturbation theory, compression, and numerical evaluation of the time-ordered product to explore the interesting physics and numerics.

The remainder of the paper is organized as follows: In Sec. II, we introduce the Landau–Zener problem and discuss the Pauli spin matrix identities needed to work with the problem. In Sec. III, we describe the discretized time evolution via the Trotter product formula. In Sec. IV, we illustrate how time-dependent perturbation theory can append the time evolution of the semi-infinite tails using the interaction picture

in a first-order expansion. Compression algorithms are discussed in Sec. V, followed by implementation strategies for the classroom and conclusions in Sec. VI.

II. THE LANDAU–ZENER PROBLEM AND PAULI SPIN-MATRIX IDENTITIES

The Landau–Zener problem consists of determining the probability to transition from the ground-state to the excited state of a two-level system, after the two states approach each other with an avoided crossing and then depart from each other. The Landau–Zener system is described by the Hamiltonian,

$$\hat{H}(t) = \begin{pmatrix} vt & \delta \\ \delta & -vt \end{pmatrix} = vt\sigma_z + \delta\sigma_x, \qquad (1)$$

where t is time, v is the rate at which the two levels approach each other, and δ is the coupling between them that determines the minimal energy gap (2δ) of the avoided crossing (occurring at time $t = 0$). Both v and δ are real numbers with units of energy/time and energy, respectively. The symbols σ_z and σ_x represent Pauli spin matrices,

$$\sigma_x = \begin{pmatrix} 0 & 1 \\ 1 & 0 \end{pmatrix}, \quad \sigma_y = \begin{pmatrix} 0 & -i \\ i & 0 \end{pmatrix}, \quad \sigma_z = \begin{pmatrix} 1 & 0 \\ 0 & -1 \end{pmatrix}. \qquad (2)$$

By diagonalizing the Landau–Zener Hamiltonian using time as a *parameter*, one obtains two instantaneous eigenenergy levels shown in Fig. 1(a). Initially, when $t = -\infty$, the two energy eigenvectors $|\psi_\pm\rangle$ given by

$$|\psi_+\rangle = \begin{pmatrix} 1 \\ 0 \end{pmatrix} \quad \text{and} \quad |\psi_-\rangle = \begin{pmatrix} 0 \\ 1 \end{pmatrix} \qquad (3)$$

are infinitely separated in energy and the system starts in the ground-state $|\psi(-\infty)\rangle = |\psi_+\rangle$. As the system evolves with time, the two levels $E_+(t)$ (the upper instantaneous energy level) and $E_-(t)$ (the lower instantaneous energy level) approach each other as $t \to 0$ and then move apart as $t \to \infty$. Because the ground state smoothly changes from $|\psi_+\rangle$ as $t \to -\infty$ to $|\psi_-\rangle$ as $t \to \infty$, the probability to remain in the ground state for large positive times is given by $P_-(t) = |\langle\psi_-|\psi(t)\rangle|^2$. Similarly, the probability to end in the excited state at long times is given by $P_+(t) = 1 - P_-(t) = |\langle\psi_+|\psi(t)\rangle|^2$. We are interested in both of these probabilities when $t \to \infty$, $P_+(\infty)$ and $P_-(\infty)$.

As shown in Fig. 1(a), to transition from the lower-energy state to the higher-energy state, when traversing the avoided crossing, the system has to tunnel through a gap of size at least 2δ, so the probability to transition is associated with a tunneling process. Depending on the value of the rate v and the level separation δ, we distinguish between two types of transitions. If the system evolves adiabatically, that is, extremely slowly, it will always remain in the lower-energy state (the lower band); that is, it will make perfect transitions from one instantaneous ground state to another along its time evolution. According to the diagram in Fig. 1(a) this means that around $t = 0$ there will be a slow and smooth transition from $|\psi_+\rangle$ to $|\psi_-\rangle$. If we let the system evolve diabatically (fast), it tunnels from the lower to the upper band. The
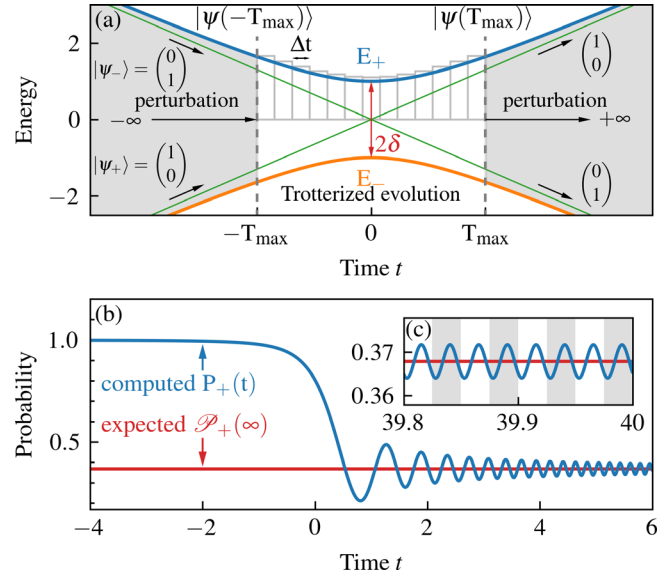

Fig. 1. (Color online) Landau–Zener system: (a) Time evolution of the two instantaneous eigenenergy levels $E_\pm(t) = \pm\sqrt{v^2 t^2 + \delta^2}$ (the upper blue and the lower orange curve). At time $t = 0$, the two levels are separated by the minimal energy gap of $E_+(0) - E_-(0) = 2\delta$. The green lines show the crossing of the ($\delta = 0$) energy levels $\pm vt$ at time $t = 0$ in a system that has no coupling between the levels. The time evolution algorithm that we use is divided into three parts. The initial state $|\psi(-T_{max})\rangle$ is obtained either using perturbation theory applied to $|\psi_+\rangle$ at $t = -\infty$ (what we consider as *the perturbed state*) or is set to $|\psi_+\rangle$ at $-T_{max}$ (what we consider as *the unperturbed initial state*). This initial state is then propagated towards $|\psi(T_{max})\rangle$ using an evolution operator in the Trotterized form with a time step of Δt. An additional perturbation is applied to $|\psi(T_{max})\rangle$ to obtain the final state at $t = +\infty$, or $|\psi(T_{max})\rangle$ is considered to be the final state (for the two different types of calculations). (b) Time evolution of the computed transition probability $P_+(t) = |\langle\psi_+|\psi(t)\rangle|^2$ compared to the expected probability $\mathscr{P}_+(\infty)$ obtained from the analytical expression for the Landau–Zener transition. The rate is $v = \pi$ and $\delta = 1$; we use these same parameters for all of the numerical calculations in this paper. The inset in panel (c) shows the fast oscillations of the transition probability $P_+(t)$ with time on a backdrop of width $vt^2 = 4N\pi$ (gray and white background), showing that these oscillations have a period proportional to $\sim t^2$. The amplitude of these oscillations for the interval $[-T_{max}, T_{max}]$ decays quite slowly with T_{max} (as a power law) unless corrected by the time-dependent perturbation theory.

objective of the Landau–Zener calculation is to precisely determine these probabilities as functions of v and δ.

Zener[2] solved the full time-dependent problem analytically by mapping the equation of motion of the system into the form of the Weber equation, which allowed him to obtain the exact solution $\mathscr{P}_+(\infty) = \exp(-\pi\delta^2/\hbar v)$. Here, we present a computational approach to find the same solution numerically.

The first issue that arises when considering this problem from a numerical perspective is how to deal with the infinite times. Numerical simulations work with finite times, so how does one effectively start with a state at $t = -\infty$ and obtain a result at $t = +\infty$ on a computer? It is usually assumed that starting in the state $|\psi_+\rangle$ at some sufficiently large (but finite) negative time is justified and will lead to an accurate numerical solution. However, the Landau–Zener problem is known for its slowly decaying oscillations of the transition probability $P_+(t)$ with time, which are illustrated on the right hand side of Fig. 1(b) and in Fig. 1(c). Although the time evolution of a two-level system is a simple problem to solve numerically and is not computationally demanding, the persistence of these slowly decaying oscillations presents a

serious problem in accurately determining the transition probability as $t \to \infty$. This problem might seem trivial here, since the analytical solution is known, but it becomes important for generalizations of the Landau–Zener problem, where the level separation is not linear in time and the exact solution is not known. In our numerical approach, we show how the time evolution can be divided into three parts, where propagation from $-\infty$ to some cutoff time and from another cutoff time to $+\infty$ can be resolved using time-dependent perturbation theory (see the gray areas in Fig. 1(a)), whereas the evolution on the finite time interval between the cutoffs can be computed using the Trotter product formula, which discretizes the time evolution operator. We discuss both these approaches in more detail in Secs. III–VI.

Before we explain how to implement these quantum-mechanical concepts, we have to establish some mathematical prerequisites necessary to understand time evolution in quantum mechanics and time-ordered products of Hamiltonians based on Pauli matrices (two-level systems). Pauli matrices satisfy the commutation relations,

$$[\sigma_i, \sigma_j] = \sigma_i \sigma_j - \sigma_j \sigma_i = 2i \sum_k \varepsilon_{ijk} \sigma_k, \tag{4}$$

where the indices i, j and k represent the coordinates x, y, and z, the factor $2i$ is twice the imaginary number i, and ε_{ijk} is the Levi-Civita (completely antisymmetric) tensor; this is a tensor that is equal to 1 when ijk is an even permutation of 123, is equal to –1 when ijk is an odd permutation of 123, and vanishes otherwise. Similarly, their anticommutator is given by

$$\{\sigma_i, \sigma_j\} = \sigma_i \sigma_j + \sigma_j \sigma_i = 2\delta_{ij} \mathbb{I}, \tag{5}$$

where $\mathbb{I}$ is the unit matrix and δ_{ij} is the Kronecker delta function. These two expressions can be combined to create the product formula for any two Pauli matrices,

$$\sigma_i \sigma_j = \delta_{ij} \mathbb{I} + i \sum_k \varepsilon_{ijk} \sigma_k. \tag{6}$$

The product formula is useful for evaluating the exponentials of weighted sums of Pauli matrices, which are needed to construct the time evolution operators. The exponential of a linear combination of Pauli matrices can be expanded into an infinite series

$$e^{i\vec{\gamma} \cdot \vec{\sigma}} = \sum_{n=0}^{\infty} \frac{(i\vec{\gamma} \cdot \vec{\sigma})^n}{n!}. \tag{7}$$

Here, $\vec{\gamma}$ is a 3-component vector of real numbers and the dot product is understood as $\vec{\gamma} \cdot \vec{\sigma} = \gamma_x \sigma_x + \gamma_y \sigma_y + \gamma_z \sigma_z$ (which is a 2×2 matrix). The quadratic term $(i\vec{\gamma} \cdot \vec{\sigma})^2$ in the series is computed by using the product formula for two Pauli matrices. One obtains

$$(i\vec{\gamma} \cdot \vec{\sigma})^2 = -\sum_i \sum_j \gamma_i \gamma_j \sigma_i \sigma_j = -\sum_i \gamma_i \gamma_i \mathbb{I} = -|\vec{\gamma}|^2 \mathbb{I}. \tag{8}$$

Here, the $\sum_{ij} \varepsilon_{ijk} \gamma_i \gamma_j \sigma_k$ term is zero because one can interchange the i and j indices in the summation and show that $\varepsilon_{ijk} \gamma_i \gamma_j \sigma_k = -\varepsilon_{ijk} \gamma_i \gamma_j \sigma_k$. The infinite sum can then be broken into two sums—those involving even powers and those involving odd powers. Each can be resummed to yield $\cos|\vec{\gamma}|$ or $\sin|\vec{\gamma}|$. This simplification yields the generalized Euler identity for Pauli matrices,

$$e^{i\vec{\gamma} \cdot \vec{\sigma}} = \cos|\vec{\gamma}| \, \mathbb{I} + i \sin|\vec{\gamma}| \frac{\vec{\gamma} \cdot \vec{\sigma}}{|\vec{\gamma}|}, \tag{9}$$

which transforms the symbolic expression for an exponential of the Pauli matrices into a concrete 2×2 matrix. This result will be employed in computing the time-evolution operator. We also use the product formula of two Pauli matrices to compute the product of two exponentials of linear combinations of Pauli matrices via

$$\begin{aligned}
e^{i\vec{\gamma} \cdot \vec{\sigma}} e^{i\vec{\gamma}' \cdot \vec{\sigma}} = &\left(\cos|\vec{\gamma}| \cos|\vec{\gamma}'| - \sin|\vec{\gamma}| \sin|\vec{\gamma}'| \frac{\vec{\gamma} \cdot \vec{\gamma}'}{|\vec{\gamma}||\vec{\gamma}'|} \right) \mathbb{I} \\
&+ i \left(\cos|\vec{\gamma}| \sin|\vec{\gamma}'| \frac{\vec{\gamma}'}{|\vec{\gamma}'|} + \sin|\vec{\gamma}| \cos|\vec{\gamma}'| \frac{\vec{\gamma}}{|\vec{\gamma}|} \right. \\
&\left. - \sin|\vec{\gamma}| \sin|\vec{\gamma}'| \frac{\vec{\gamma} \times \vec{\gamma}'}{|\vec{\gamma}||\vec{\gamma}'|} \right) \cdot \vec{\sigma}.
\end{aligned} \tag{10}$$

It is important to emphasize that, unlike exponentials of real numbers, the expression $e^{i\vec{\gamma} \cdot \vec{\sigma}} e^{i\vec{\gamma}' \cdot \vec{\sigma}} = e^{i(\vec{\gamma} + \vec{\gamma}') \cdot \vec{\sigma}}$ does not generally apply for exponentials of Pauli matrices. The reason for this is the last term in Eq. (10) with the scalar triple product. When this term is present, the product of the two exponentials does not commute and they cannot be interchanged. In the case when two vectors $\vec{\gamma}$ and $\vec{\gamma}'$ are colinear, then the triple-product term vanishes, the two coefficients can be summed, and the two exponentials do commute.

III. COMPUTATIONAL APPROACHES TO THE TIME-ORDERED PRODUCT

Regardless of how we propagate from $t = -\infty$ to $t = -T_{\max}$ (and $t = T_{\max}$ to $t = \infty$), we still must use the computer to explicitly propagate from $t = -T_{\max}$ to $t = T_{\max}$. To time evolve the state $|\psi(-T_{\max})\rangle$ to the state $|\psi(T_{\max})\rangle$, we must apply the appropriate time-evolution operator. The time-evolution operator satisfies

$$|\psi(t)\rangle = \hat{U}(t, t_0)|\psi(t_0)\rangle \tag{11}$$

and depends on the initial time t_0 and the final time t. The time-evolution operator can be found from the facts that it must be unitary (so that it preserves the norm of the state at any time $|\langle \psi(t)|\psi(t)\rangle|^2 = 1$) and that it must have the "semigroup property," which implies that time evolution is additive. In other words, evolving the state from $t_0 \to t'$ and from $t' \to t$ is the same as directly evolving the state from $t_0 \to t$. Since the Hamiltonian must govern the time evolution, we are led to $\hat{U}(t, t_0) = e^{-(i/\hbar)(t-t_0)\hat{H}}$ for time-independent Hamiltonians because the sign in the exponent is determined by convention.

In the time-dependent case, we determine the full evolution operator by considering the time evolution over a short time interval from t to $t + \Delta t$. We simply assume that the time interval is short enough that we can take $\hat{H}(t)$ as being piecewise constant (over the time interval of length Δt) and use the constant Hamiltonian time evolution operator for this

piecewise constant Hamiltonian over the short interval Δt. Then,

$$\hat{U}(t + \Delta t, t) = e^{-(i/\hbar)\hat{H}(t)\Delta t}. \tag{12}$$

By applying a sequence of these operators one can construct a discretized version of the evolution operator,

$$\hat{U}(t, t_0) = \hat{U}(t, t - \Delta t)\hat{U}(t - \Delta t, t - 2\Delta t) \cdots$$
$$\cdots \hat{U}(t_0 + 2\Delta t, t_0 + \Delta t)\hat{U}(t_0 + \Delta t, t_0), \tag{13}$$

which approaches the exact evolution operator as $\Delta t \to 0$. This is called the Trotter product formula. In the limit of $\Delta t \to 0$, the time-ordered product is conventionally written as

$$\hat{U}(t, t_0) = \mathscr{T}\left[\exp\left(-\frac{i}{\hbar}\int_{t_0}^{t}\hat{H}(t')dt'\right)\right], \tag{14}$$

where $\mathscr{T}$ is the time-ordering operator, which orders times with the "latest times to the left."

In our numerical approach to the Landau–Zener problem, the time evolution over the finite interval $-T_{\max} \leq t \leq T_{\max}$ is performed via the Trotter product formula with the time step Δt. We write the evolution operator $\hat{U}(T_{\max}, -T_{\max})$ as a time-ordered sequence of exponentials of the Landau–Zener Hamiltonian

$$\hat{U}(t + \Delta t, t) = e^{-(i/\hbar)(vt\sigma_z + \delta\sigma_x)\Delta t}$$
$$= \cos\left(\sqrt{v^2t^2 + \delta^2}\,\frac{\Delta t}{\hbar}\right)\mathbb{I}$$
$$-i\frac{\sin\left(\sqrt{v^2t^2 + \delta^2}\,\dfrac{\Delta t}{\hbar}\right)}{\sqrt{v^2t^2 + \delta^2}\,\dfrac{\Delta t}{\hbar}}(vt\sigma_z + \delta\sigma_x)\frac{\Delta t}{\hbar}, \tag{15}$$

after using the generalized Euler identity for the exponentials of the Pauli matrices in Eq. (9). Each of the exponential Trotter factors $U(t + \Delta t, t)$ is now a concrete 2×2 matrix that acts on the state at a given time. Here, we use the exponentiated linear superposition of Pauli matrices with the vector $\vec{\gamma} = -(\Delta t/\hbar)(vt, 0, \delta)$ (which is a time-dependent vector) for each Trotter factor. Note that, in general, $\exp[i(a\sigma_z + b\sigma_x)] \neq \exp(ia\sigma_z)\exp(ib\sigma_x)$ because the matrices σ_z and σ_x do not commute, as explained in Sec. II. However, if the coefficients a and b are very small, as in the case of Eq. (15) for $\Delta t \to 0$, then $\exp[i(a\sigma_z + b\sigma_x)] \approx \exp(ia\sigma_z)\exp(ib\sigma_x)$ because the error corresponding to the commutator of the two terms is on the order of $\sim\Delta t^2$. Thus, if the evolution operator is written in the Trotter product form, when Δt is sufficiently small, one can approximate a Trotter factor via

$$\hat{U}(t + \Delta t, t) \approx e^{(i/\hbar)vt\sigma_z\Delta t}e^{-(i/\hbar)\delta\sigma_x\Delta t}, \tag{16}$$

which we call the *split*-form of the evolution operator. We contrast this to the evolution operator in Eq. (15), that we call the *exact* form since there is no approximation (except assuming the Hamiltonian is constant over the time interval Δt). The evolution operator expressed in the split form is accurate to the order of Δt^2, so the two forms should approach one another in the limit of $\Delta t \to 0$.

The operator in the split form has an additional interesting feature. The exponentials of the σ_x matrix $\exp(-(i/\hbar)\delta\sigma_x\Delta t)$ in the Trotter product sequence are constant for a fixed time step Δt, whereas the σ_z terms $\exp(-(i/\hbar)vt\sigma_z\Delta t)$ depend on time t. At special times, T_n, the exponent will satisfy the condition $vT_n\Delta t/\hbar = 2n\pi$. At these times, the given Trotter component with σ_z (in the split form) is a unit matrix. The next σ_z component in the Trotter product will have the exponent $v(T_n + \Delta t)\Delta t/\hbar$, which is the same as the earlier term $v(T_{n-1} + \Delta t)\Delta t/\hbar$ and the same as the even earlier time $v\Delta t\Delta t/\hbar$, and so on. This means that in the split form, the Trotter product repeats with period $T = 2\pi\hbar/(v\Delta t)$. However, we know that the exact time evolution operator is not periodic. Thus, this periodicity is an artifact of using the split form. It means that we must choose a Δt such that the split form is not close to its periodic behavior over the interval $-T_{\max} \leq t \leq T_{\max}$. If we do not, then the accumulation of error in the split form leads to the transition probability repeatedly switching between $P_+(-T/2)$ and $P_+(T/2)$ as time passes through different T_n points. To obtain precise results using the split method, we should pick Δt so that $T > T_{\max}$, ideally $T_{\max}$ no larger than one fourth of the period $T/4$.

We now discuss how to perform the numerical calculation. The time evolution can be implemented in two different ways. One can write a function that computes the time-evolution operator $\hat{U}(t + \Delta t, t)$ at every time step and applies it to the state $|\psi(t)\rangle$ to obtain $|\psi(t + \Delta t)\rangle$ (propagating the state), or one can multiply this time-evolution operator with the accumulated time-evolution operator for all previous times $\hat{U}(t + \Delta t, -T_{\max}) = \hat{U}(t + \Delta t, t)\hat{U}(t, -T_{\max})$ (propagating the operator). In the latter case, the state is obtained from $|\psi(t + \Delta t)\rangle = \hat{U}(t + \Delta t, -T_{\max})|\psi(-T_{\max})\rangle$.

Using the Trotter product formula combined with the generalized Euler identity for each Trotter factor enables the numerical solution of the Landau–Zener problem on the finite time interval $[-T_{\max}, T_{\max}]$. Since we are working with 2×2 matrices that have an explicit form for each time step, this time evolution is relatively straightforward to program. However, we still need to determine the initial state $|\psi(-T_{\max})\rangle$. In Sec. IV, we explain how to include the time evolution operator over the two semi-infinite intervals by using the interaction picture and the time-dependent perturbation theory.

IV. EXTRAPOLATION TO INFINITE TIME WITH TIME-DEPENDENT PERTURBATION THEORY

The roadblock to analytically determining the evolution operator for the Landau–Zener problem in Eq. (1) is the linear time dependence of the σ_z term and the fact that the two Pauli matrices (σ_z and σ_x) do not commute. This makes the time-ordered product in Eq. (14) virtually impossible to solve analytically.

For large positive and negative times, we must use time-dependent perturbation theory. However, while in conventional quantum instruction, the unperturbed Hamiltonian is always chosen to be the time independent piece and the perturbation is time dependent, here, the unperturbed part of the Hamiltonian is the large piece (the σ_z piece for large $|t|$), and the perturbation is the constant piece (the σ_x piece). So, we split the Landau–Zener Hamiltonian into two parts: The main time-dependent Hamiltonian $\hat{H}_0(t) = vt\sigma_z$ and the time-independent perturbation $\hat{V} = \delta\sigma_x$. The evolution operator is then constructed in the interaction picture via

$$\hat{U}(t, t_0) = \hat{U}_0(t, t_0)\hat{U}_I(t, t_0)$$

$$= \hat{U}_0(t, t_0)\mathscr{T}\left[e^{-\frac{i}{\hbar}\int_{t_0}^{t}\hat{V}_I(t')dt'}\right], \quad (17)$$

where $\hat{U}_0(t, t_0)$ is the evolution operator for the unperturbed Hamiltonian $\hat{H}_0(t)$, and $\hat{U}_I(t, t_0)$ is the evolution operator for the perturbation. In the interaction picture, we have $\hat{V}_I(t) = \hat{U}_0^\dagger(t, t_0)\hat{V}\hat{U}_0(t, t_0)$. The time ordered product $\mathscr{T}$ in Eq. (17) is to be understood in the same sense as in Eq. (14), meaning that we write it as an ordered sequence of exponentials of each term in the integrand $\hat{V}_I(t)$. Note that Eq. (17) is typically not the exponential of the integral of the operator $\hat{V}_I(t)$; this only occurs if the integrand commutes with itself for different times. Note further that the notion of time-dependent perturbation theory here arises because as t goes to $\pm\infty$, the unperturbed piece $\hat{H}_0(t)$ is much larger than $\hat{V}$. We also emphasize that Eq. (17) is exact and does not contain any approximation (the perturbative approximation arises from Taylor expanding the evolution operator $\hat{U}_I(t, t_0)$ as we show below).

The evolution operator for the unperturbed Hamiltonian $\hat{H}_0(t)$ can be computed analytically because it commutes with itself for all times. Hence, we can just integrate the unperturbed piece to find $\hat{U}_0(t, t_0) = e^{-(i/\hbar)(1/2)v(t^2-t_0^2)\sigma_z}$. We next use this exact result to determine the perturbation in the interaction picture (which is a rotation of the σ_x matrix about the z-axis). It becomes

$$\hat{V}_I(t) = e^{\frac{i}{\hbar}\frac{1}{2}v(t^2-t_0^2)\sigma_z}\delta\sigma_x e^{-\frac{i}{\hbar}\frac{1}{2}v(t^2-t_0^2)\sigma_z}$$

$$= \delta\left(\sigma_x\cos\frac{v(t^2-t_0^2)}{\hbar} - \sigma_y\sin\frac{v(t^2-t_0^2)}{\hbar}\right), \quad (18)$$

which can be found by using the generalized Euler identity to determine each exponential factor and then multiplying the three matrices together. The strategy of perturbation theory is to approximate the time-ordered product for $\hat{U}_I(t, t_0)$ in the evolution operator by

$$\hat{U}(t, t_0) \approx \hat{U}_0(t, t_0)\left(\mathbb{I} - \frac{i}{\hbar}\int_{t_0}^{t}\hat{V}_I(t')dt'\right), \quad (19)$$

which is accurate for t close to t_0, or when $\hat{V}_I$ is "small." Directly computing the $\hat{V}_I(t)$ operator from Eq. (18) and then factoring the result in terms of Pauli matrices gives

$$\hat{V}_I(t') = \begin{pmatrix} 0 & e^{(i/\hbar)v(t'^2-t_0^2)} \\ e^{-(i/\hbar)v(t'^2-t_0^2)} & 0 \end{pmatrix},$$

$$= e^{-\frac{i}{\hbar}\frac{1}{2}vt_0^2\sigma_z}\begin{pmatrix} 0 & e^{(i/\hbar)vt'^2} \\ e^{-(i/\hbar)vt'^2} & 0 \end{pmatrix}$$

$$\times e^{\frac{i}{\hbar}\frac{1}{2}vt_0^2\sigma_z},$$

$$= \hat{Z}(t_0)\hat{V}_I'(t')\hat{Z}^{-1}(t_0), \quad (20)$$

where $\hat{Z}(t) = e^{-(i/\hbar)(1/2)vt^2\sigma_z}$. The unit matrix can also be written as $\mathbb{I} = \hat{Z}(t_0)\mathbb{I}\hat{Z}^{-1}(t_0)$ and $\hat{U}_0(t, t_0) = \hat{Z}(t)\hat{Z}^{-1}(t_0)$, so the evolution operator becomes

$$\hat{U}(t, t_0) \approx \hat{Z}(t)\hat{Z}^{-1}(t_0)\left[\hat{Z}(t_0)\mathbb{I}\hat{Z}^{-1}(t_0) - \frac{i}{\hbar}\hat{Z}(t_0)\right.$$

$$\times \left. \int_{t_0}^{t}\hat{V}_I'(t')dt'\hat{Z}^{-1}(t_0)\right]$$

$$= \hat{Z}(t)\left[\mathbb{I} - \frac{i}{\hbar}\int_{t_0}^{t}\hat{V}_I'(t')dt'\right]\hat{Z}^{-1}(t_0). \quad (21)$$

Equation (21) yields an approximate formula for the evolution operator in the interaction picture for any two times. We now apply it to compute $\hat{U}(-T_{\max}, -\infty)$ and $\hat{U}(+\infty, T_{\max})$. In the first case, the operator $\hat{Z}^{-1}(t_0 = -\infty)$ on the right side of Eq. (21) can be neglected because we start from an eigenstate of the σ_z operator (the $|\psi_+\rangle$ state) and acting with $\hat{Z}^{-1}$ will just produce a global complex phase, which does not affect the probabilities. In the second case, when computing $\hat{U}(+\infty, T_{\max})$ the operator on the left side of Eq. (21) (i.e., $\hat{Z}(t = \infty)$) can be neglected because we are interested only in the probability $P_+(\infty)$ and that term also just contributes a complex phase, which cancels out. The matrix integral in Eq. (21) can be analytically computed in both cases. For $\hat{U}(-T_{\max}, -\infty)$ it equals

$$\mathbb{I} - \frac{i}{\hbar}\int_{-\infty}^{-T_{\max}}\hat{V}_I'(t')dt' = \begin{pmatrix} 1 & -\frac{i}{\hbar}\xi(T_{\max}) \\ -\frac{i}{\hbar}\eta(T_{\max}) & 1 \end{pmatrix}, \quad (22)$$

where

$$\eta(t) = \sqrt{\frac{\pi}{2v}}\frac{(i-1)}{2}\left[1 - \text{erf}\left(\sqrt{\frac{v}{2}}(i+1)t\right)\right], \quad (23)$$

and

$$\xi(t) = \sqrt{\frac{\pi}{2v}}\frac{(i+1)}{2}\left[1 + \text{erf}\left(\sqrt{\frac{v}{2}}(i-1)t\right)\right]. \quad (24)$$

Both off-diagonal components of the perturbation matrix, $\eta(t)$ and $\xi(t)$, are expressed in terms of the error function

$$\text{erf}(z) = \frac{2}{\sqrt{\pi}}\int_0^z e^{-t^2}dt, \quad (25)$$

with a complex argument. The evolution operator obtained through perturbation theory is approximate and not necessarily unitary. This means the quantum state must be normalized "by hand" after applying the approximate evolution operator. In other words, we renormalize both at time $t = -T_{\max}$ and at $t = \infty$. Note that the central integral in Eq. (21) does not change for $\hat{U}(+\infty, T_{\max})$, which follows from $\hat{V}_I'(-t) = \hat{V}_I'(t)$ and from the change of variables $t' \rightarrow -t'$, but the $\hat{Z}(t)$ and $\hat{Z}^{-1}(t_0)$ operators do change.

The improvement in accuracy for the calculation that includes the time-dependent perturbation theory arises from its use of a more accurate initial state at $-T_{\max}$. This improvement is shown in Fig. 2. In Fig. 2(a), we compare the phase of the state $|\psi(t)\rangle$ obtained by propagating $|\psi_+\rangle$ from a distant time $-T_{\max} = -1000$ (blue curve) with the
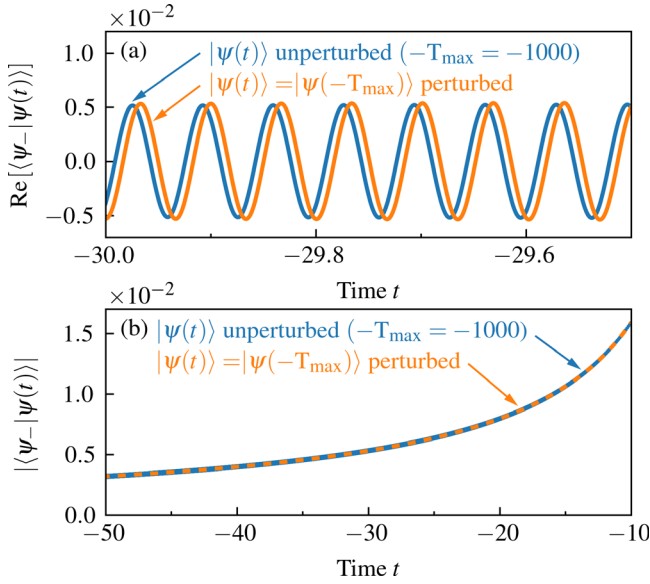
Fig. 2. (Color online) State evolution for different starting conditions: (a) the real part of the projected wave function $\mathrm{Re}[\langle\psi_-|\psi(t)\rangle]$ for the initial state computed as a function of time using perturbation theory $|\psi(t)\rangle = |\psi(-T_{\max})\rangle$ (orange curve) vs the unperturbed state $|\psi(t)\rangle$ computed by the time evolution from $|\psi_+\rangle$ starting at $-T_{\max} = -1000$ (blue curve). (b) Time evolution of the modulus of the state projection $|\langle\psi_-|\psi(t)\rangle|$ computed for the same two starting conditions as in panel (a).

one obtained by perturbation theory as functions of time ($t = T_{\max}$, the orange curve). In general, the amplitude $|\langle\psi_-|\psi(t)\rangle|$ in Fig. 2(b) matches the perturbed and unperturbed state, but as shown in Fig. 2(a) they differ by a phase. This initial phase difference introduces an error for later times that propagates through the Trotter product. The advantage of the perturbation theory is that it reduces the computational demand by reducing the time range $[-T_{\max}, T_{\max}]$ needed for the numerical calculation. Instead of propagating the state from a very distant past, one can obtain a precise result for a much smaller $T_{\max}$. The perturbation that brings the state to $t = +\infty$ is even more important, because it removes the small but persistent oscillations of the transition probability, as we show in Sec. VI. Note that discussing time-dependent perturbation theory provides a number of benefits to the students: (i) it shows them how to extrapolate solutions from finite to infinite time; (ii) it illustrates how to employ time-dependent perturbation theory in a nonstandard fashion; and (iii) it shows how small errors in the initial conditions can propagate in a calculation and affect results at later times if they are not properly addressed.

V. COMPRESSION ALGORITHMS

In Sec. III, we explained how to compute the time evolution operator with the Trotter product and time discretization. Using the generalized Euler identity, the exponents at each time step can be converted into 2×2 matrices and the evolution operator can be computed by matrix multiplication. Replacing a sequence of exponentiated operators (as in the Trotter product) with a single exponential operator is called *compression*. Sophisticated compression algorithms based on the Cartan decomposition of Lie groups are employed in quantum computing to greatly reduce the depth of circuits.[3,4] In this section, we show how a simpler application using the two equivalent ways to represent rotations can be used to

compress the time-evolution operator that we use in the Landau–Zener problem, which provides a nice opportunity to show how compression algorithms work in a quantum class.

Instead of computing the evolution operator by matrix multiplication for each time step, compression relies on combining the exponential parameters (the vectors $\vec{\gamma}$ used in each exponential $e^{i\vec{\gamma}\cdot\vec{\sigma}}$ factor) into a single vector, for the evolution operator over the finite time interval. The basic idea for compression comes from the fact that each exponent of a Pauli matrix represents a rotation on the Bloch sphere. A sequence of rotations about different axes can be replaced by a single rotation around a single axis. We focus on two compression algorithms that could be used to compute the evolution operator $\hat{U}(T_{\max}, -T_{\max})$.

The first algorithm is called *XZX* compression and it is based on a mathematical relationship between the Pauli matrices

$$e^{-i\alpha\sigma_x}e^{-i\beta\sigma_z}e^{-i\gamma\sigma_x} = e^{-ia\sigma_z}e^{-ib\sigma_x}e^{-ic\sigma_z}, \quad (26)$$

where one can compute a, b, and c from the known coefficients α, β, and γ. With the help of the generalized Euler identity, we convert the left and the right side of Eq. (26) into 2×2 matrices and compute the relationships between the coefficients by equating the four matrix elements of the final products on each side of the equation. This gives exact inverse trigonometric relations,

$$a = \frac{1}{2}\arctan\left[\tan(\beta)\frac{\cos(\alpha-\gamma)}{\cos(\alpha+\gamma)}\right]$$
$$- \frac{1}{2}\arctan\left[\tan(\beta)\frac{\sin(\alpha-\gamma)}{\sin(\alpha+\gamma)}\right], \quad (27)$$

$$b = \arctan\left[\sqrt{\frac{\sin^2(\alpha+\gamma) + \tan^2(\beta)\sin^2(\alpha-\gamma)}{\cos^2(\alpha+\gamma) + \tan^2(\beta)\cos^2(\alpha-\gamma)}}\right], \quad (28)$$

$$c = \frac{1}{2}\arctan\left[\tan(\beta)\frac{\cos(\alpha-\gamma)}{\cos(\alpha+\gamma)}\right]$$
$$+ \frac{1}{2}\arctan\left[\tan(\beta)\frac{\sin(\alpha-\gamma)}{\sin(\alpha+\gamma)}\right]. \quad (29)$$

As shown in Fig. 3(a), the identity in Eq. (26) can be applied to the time evolution operator for the Landau–Zener problem written as a Trotter product in the split-form in Eq. (16). Here, the Trotter product is a sequence of alternating constant σ_x and time-dependent σ_z exponentials (the first row of Fig. 3(a)). Taking the three exponentials lying inside the red box in the first row of Fig. 3(a), we apply Eq. (26) and switch the ordering of the operators to the one in the second row of Fig. 3(a); that is, we change a product of exponentials in the form *XZX* into the form *ZXZ*. This re-expression of factors allows the now adjacent σ_z exponentials on the edges of the red box on the second line to merge into a single exponential as emphasized by the red boxes in the third row of Fig. 3(a). The initial five exponential components are then compressed into three. This procedure is repeated until the Trotter product is reduced to just three exponential factors, which can each be computed using the generalized Euler formula.

The second compression algorithm is computationally far more efficient than the *XZX* compression since it does not

(a) XZX compression
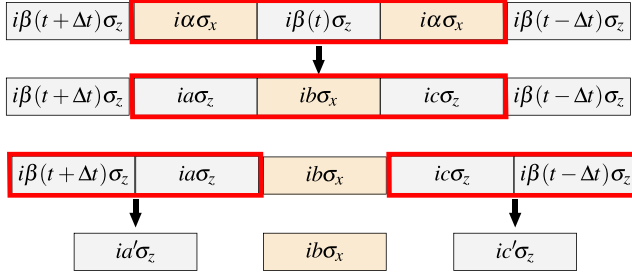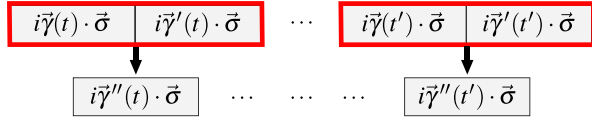

(b) nearest neighbor compression

Fig. 3. (Color online) Schematics of the two possible compression algorithms of the Trotterized evolution operator. The boxes represent exponential coefficients at every Trotter step. (a) XZX compression, where a $\sigma_x\sigma_z\sigma_x$ sequence of the evolution operator exponentials in the Trotter-split form is replaced with $\sigma_z\sigma_x\sigma_z$ sequence, so that neighboring σ_z components can be merged together. (b) The nearest neighbor compression method, where two neighboring Trotter components of the evolution operator (based on the exact Hamiltonian) are merged together at every compression step.

require any inverse trigonometric functions. We call this algorithm the nearest-neighbor algorithm because it involves merging the neighboring exponentials in the Trotter product as shown in Fig. 3(b). In contrast to the XZX compression, which requires the split form of the Trotter product, the nearest-neighbor compression uses an exact form for each Trotter factor. This compression algorithm is based on Eq. (10) for the product of two exponentials $e^{i\vec{\gamma}\cdot\vec{\sigma}}e^{i\vec{\gamma}'\cdot\vec{\sigma}} = e^{i\vec{\gamma}''\cdot\vec{\sigma}}$. We simply need to construct the vector $\vec{\gamma}''$ from the known $\vec{\gamma}$ and $\vec{\gamma}'$. Comparing the generalized Euler formula in Eq. (9) and its extension to a product of two exponentials in Eq. (10), we immediately find that

$$\cos|\vec{\gamma}''| = \cos|\vec{\gamma}|\cos|\vec{\gamma}'| - \sin|\vec{\gamma}|\sin|\vec{\gamma}'|\frac{\vec{\gamma}\cdot\vec{\gamma}'}{|\vec{\gamma}||\vec{\gamma}'|}, \quad (30)$$

and

$$\sin|\vec{\gamma}''|\frac{\vec{\gamma}''}{|\vec{\gamma}''|} = \left(\cos|\vec{\gamma}|\sin|\vec{\gamma}'|\frac{\vec{\gamma}'}{|\vec{\gamma}'|} + \sin|\vec{\gamma}|\cos|\vec{\gamma}'|\frac{\vec{\gamma}}{|\vec{\gamma}|}\right.$$
$$\left. -\sin|\vec{\gamma}|\sin|\vec{\gamma}'|\frac{\vec{\gamma}\times\vec{\gamma}'}{|\vec{\gamma}||\vec{\gamma}'|}\right). \quad (31)$$

The previous two equations connects both the four-component vector $(\cos|\vec{\gamma}|, \sin|\vec{\gamma}|(\vec{\gamma}/|\vec{\gamma}|))$ for $\vec{\gamma}$ and the one for $\vec{\gamma}'$ with the one for $\vec{\gamma}''$. Nearest-neighbor compression consists in computing these four-component vectors for every step in the Trotter product and combining them using Eqs. (30) and (31). If the time interval $[-T_{\max}, T_{\max}]$ is divided into 2^{N_c} time steps, then the compression can reduce the Trotter product to a single exponential in N_c iterations (a logarithmic number of steps). Computationally, this method is much faster than XZX compression and even the direct matrix multiplication, but it requires a large amount of RAM memory for a small time step Δt because the four-component vectors are kept in memory for every time step,

whereas in the direct multiplication, the evolution operator is computed "on the fly," which requires storing only its current value. The memory requirement can be reduced if the integration interval $[-T_{\max}, T_{\max}]$ is divided into smaller intervals and compression is applied to each one of them sequentially.

There are two benefits of this work for the students. First, they learn about the idea of compression, which is becoming increasingly important in quantum computing and second, they learn how one can revise initial algorithms to make them computationally more efficient, an important skill of the computational physicist.

VI. IMPLEMENTATION STRATEGIES AND CONCLUSION

With these technical details completed, we now discuss how to implement this problem as a class project. Figure 4 shows the numerical accuracy achieved using different approaches (perturbation vs. no perturbation and exact vs. split form of the evolution operator), expressed as an error ΔP in determining the transition probability at infinity on the logarithmic scale. The logarithmic scale tells how many digits of accuracy one can achieve using different approaches. The advantage of the time-dependent perturbation theory is obvious since the unperturbed result converges very slowly to the expected probability. The figure also shows how the accuracy of the split-form of the Trotter product approaches the accuracy of the exact Hamiltonian for sufficiently small Δt. The accuracy, in this case, is limited by our choice of $T_{\max} = 30$ so the computed results converge with decreasing Δt. Similarly, Fig. 5 shows how the integration range $[-T_{\max}, T_{\max}]$ influences the computed transition probability. The persistent oscillations in the unperturbed system prevent determining the transition probability beyond two or three digits of accuracy even for $T_{\max} = 1000$. The slow decay of the unperturbed error suggests that achieving higher accuracy in this case is essentially impossible, even with increasing $T_{\max}$. The perturbed results show a high accuracy even
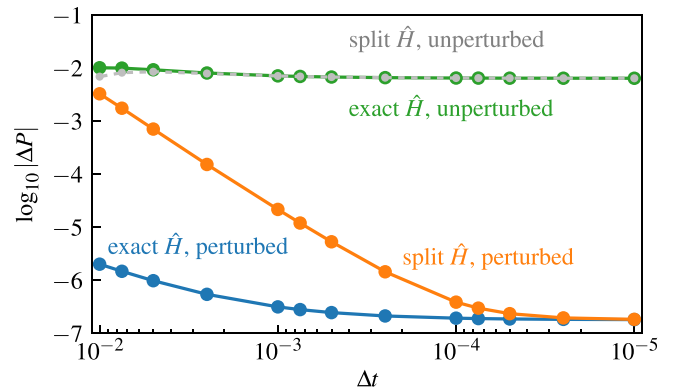

Fig. 4. (Color online) The accuracy of the computed transition probability as a function of the time step Δt. In the case of perturbed results, we compute the difference as $\Delta P = P_+(\infty) - \mathscr{P}_+(\infty)$, whereas in the case of unperturbed results we compute $\Delta P = P_+(T_{\max}) - \mathscr{P}_+(\infty)$. Here, $\mathscr{P}_+(\infty)$ is the probability obtained by the exact Landau–Zener formula $\exp(-\pi\delta^2/\hbar v)$, while $P_+(\infty)$ and $P_+(T_{\max})$ are the probabilities computed using the Trotterized evolution, with or without the perturbation, respectively. We also compare the accuracy when the Trotter step exponential is evaluated exactly, or when the Hamiltonian is split between σ_z and σ_x terms in each Trotter step. In all cases, $T_{\max} = 30$. High accuracy can only be attained for this value of $T_{\max}$ when the infinite tails are included perturbatively.
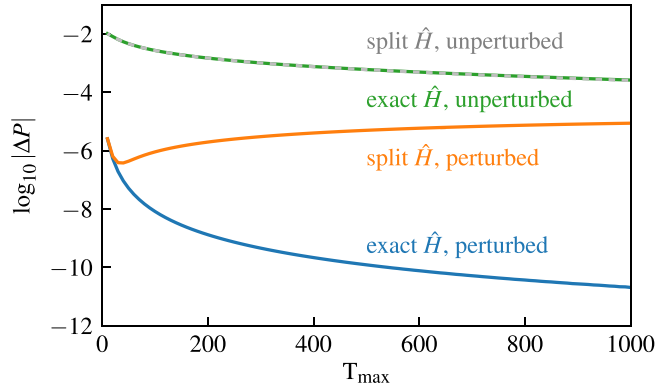
Fig. 5. (Color online) The accuracy of the computed transition probability, relative to the exact result $\exp(-\pi\delta^2/\hbar v)$, as a function of the finite time range $t \in [-T_{\max}, T_{\max}]$. The time step Δt is fixed at $\Delta t = 10^{-4}$. One expects that the time step Δt must be reduced to accurately reach larger $T_{\max}$ values because of accumulated errors. (Here, the Δt value is held *fixed*.) This clearly occurs for the split method, which is much more sensitive to Δt errors, but surprisingly is not impeding the exact, perturbed approach through nearly 12 digits of accuracy.

for small $T_{\max}$. One way to increase the accuracy in the unperturbed case is to do time-averaging once $P_+(t)$ starts to oscillate around the expected $\mathscr{P}_+(\infty)$ as done previously,[10] but it is difficult to systematically do this when the amplitude is also decreasing with time, especially to high accuracy. We also can infer how the split approximation is more sensitive to Δt errors, since we used a fixed time step, rather than reducing it as the cutoff time increases; here we see that the accumulated errors due to the finite size of the time step worsen the accuracy for large cutoff times. This advanced computational concept is beautifully illustrated in this project. Note that one need not worry about round-off error associated with matrix multiplications in this work. Those errors appear to always be much smaller than the other intrinsic errors of the computational algorithm.

The Landau–Zener problem is a challenging computational project for quantum-mechanics students, without requiring any knowledge of the higher level differential equations that are usually used to solve this problem. Students really get a taste of how computational physics works—they need to work through some nontrivial formalism to determine precisely what needs to be calculated and then they need to carefully program the results and run them. Finally, they need to examine the accuracy of the results. In the supplementary material, we provide a well-documented Python package that includes the codes used to produce the results presented in this paper. Teams can be formed to work on implementing different approaches and collaborating to compare the different outcomes (e.g., perturbation vs. no perturbation or split Trotter evolution vs. exact Trotter evolution) and discussing the computational efficiency and the numerical accuracy of each of these approaches. The workload necessary to solve this problem goes beyond a simple homework assignment, but it offers the opportunity for

students to gain deep knowledge of quantum mechanics in a practical example that will allow them to acquire skills that are important for computational research.

AUTHOR DECLARATIONS
Conflict of Interest

The authors have no conflicts to disclose.

[a] ORCID: 0000-0002-5087-0237.

[b] ORCID: 0000-0002-4655-3482.

[c] Electronic mail: james.freericks@georgetown.edu, ORCID: 0000-0002-6232-9165.

[1] L. D. Landau, "On the theory of transfer of energy at collisions II," Phys. Z. Sowjetunion **2**, 46–51 (1932).

[2] C. Zener, "Non-adiabatic crossing of energy levels," Proc. R. Soc. Lond. A **137**, 696–702 (1932).

[3] Efekan Kökcü, Daan Camps, Lindsay Bassman, J. K. Freericks, Wibe A. de Jong, Roel van Beeumen, and Alexander F. Kemper, "Algebraic compression of quantum circuits for Hamiltonian evolution," Phys. Rev. A **105**(3), 032420 (2022).

[4] Efekan Kökcü, Thomas Steckmann, Yan Wang, J. K. Freericks, Eugene F. Dumitrescu, and Alexander F. Kemper, "Fixed depth Hamiltonian simulation via Cartan decomposition," Phys. Rev. Lett. **129**(7), 070501 (2022).

[5] E. C. G. Stueckelberg, "Theorie der unelastischen Stösse zwischen atomen," Helv. Phys. Acta **5**, 369–422 (1932); available at https://www.e-periodica.ch/digbib/view?pid=hpa-001%3A1932%3A5%3A%3A149#374

[6] E. Majorana, "Atomi orientati in campo magnetico variabile," Il Nuovo Cim. **9**(2), 43–50 (1932).

[7] K. Konishi and G. Pafutto, *Quantum Mechanics: A New Introduction* (Oxford U. P., Oxford, 2009), pp. 313–315.

[8] B. Zweibach, *Mastering Quantum Mechanics: Essentials, Theory, and Applications* (The MIT Press, Cambridge, 2022), pp. 969–974.

[9] Oleh V. Ivakhnenko, Sergey N. Shevchenko, and Franco Nori, "Nonadiabatic Landau-Zener-Stückelberg-Majorana transitions, dynamics, and interference," Phys. Rep. **995**, 1–89 (2023).

[10] Y.-F. Cao, L.-F. Wei, and B.-P. Hou, "Exact solutions to Landau-Zener problems by evolution operator method," Phys. Lett. A **374**(22), 2281–2285 (2010).

[11] S. Geltman and N. D. Aragon, "Model study of the Landau-Zener approximation," Am. J. Phys. **73**(11), 1050–1054 (2005).

[12] A. G. Rojo and A. M. Bloch, "The rolling sphere, the quantum spin, and a simple view of the Landau-Zener problem," Am. J. Phys. **78**(10), 1014–1022 (2010).

[13] A. C. Vutha, "A simple approach to the Landau-Zener formula," Eur. J. Phys. **31**(2), 389–392 (2010).

[14] C. Wittig, "The Landau-Zener formula," J. Phys. Chem. B **109**(17), 8428–8430 (2005).